

Petr KAWULOK , David JUREK, Ivo SCHINDLER ,  
Rostislav KAWULOK , Petr OPĚLA , Josef NĚMEC,  
Monika KAWULOKOVÁ , Stanislav RUSZ , Michal SAUER 

VŠB – Technical University of Ostrava, Faculty of Materials Science and Technology, Czech Republic

**Forming 2022**

## FORMABILITY OF INVAR 36 ALLOY AT HIGH TEMPERATURES

### ODKSZTAŁCALNOŚĆ STOPU INVAR 36 W WYSOKICH TEMPERATURACH

By using of hot tensile tests, which were performed on simulator HDS-20, the formability of Invar 36 alloy was investigated. By a special type of a tensile test, involving a continuous control heating of the tested specimens and their simultaneous load by a constant tensile force of 80 N, a nil-strength temperature of investigated alloy 1419 °C was determined. By continuous uniaxial tensile tests to rupture the strength and plastic properties of the Invar 36 alloy were determined in the wide range of deformation temperatures (from 800 °C to 1390 °C) and mean strain rates (from 0.09 s<sup>-1</sup> to 75 s<sup>-1</sup>). On the basis of obtained results the 3D maps were constructed, expressing the dependence of the contractual hot ultimate tensile strength, hot ductility and hot reduction of area of the Invar 36 alloy on the deformation temperature and on the mean strain rate. Based on the determined plastic properties, the nil-ductility temperature of the investigated alloy of 1390 °C was also determined.

**Keywords:** Invar 36 alloy, hot tensile tests, nil-strength temperature, contractual hot ultimate tensile strength, hot ductility, hot reduction of area, nil-ductility temperature

Za pomocą prób rozciągania na gorąco, które przeprowadzono na symulatorze HDS-20, zbadano odkształcalność stopu Invar 36. Przy użyciu specjalnej próby rozciągania, polegającej na ciągłym sterowanym nagrzewaniu badanych próbek i równoczesnym ich obciążeniu stałą siłą rozciągającą 80 N, wyznaczono temperaturę zerowej wytrzymałości badanego stopu, która wyniosła 1419 °C. Za pomocą ciągłych jednoosiowych prób rozciągania prowadzonych do zerwania określono właściwości wytrzymałościowe i plastyczne stopu Invar 36 w szerokim zakresie temperatur odkształcenia (od 800 °C do 1390 °C) i średnich prędkości odkształcenia (od 0,09 s<sup>-1</sup> do 75 s<sup>-1</sup>). Na podstawie uzyskanych wyników skonstruowano mapy 3D, wyrażające zależność wytrzymałości na rozciąganie na gorąco, plastyczności na gorąco i przewężenia stopu Invar 36 od temperatury odkształcenia i średniej szybkości odkształcenia. Na podstawie wyznaczonych właściwości plastycznych określono również temperaturę przejścia w stan kruchy badanego stopu wynoszącą 1390 °C.

**Słowa kluczowe:** stop Invar 36, próby rozciągania na gorąco, temperatura przejścia w stan kruchy, umowna wytrzymałość na rozciąganie na gorąco, plastyczność na gorąco, przewężenie powierzchni na gorąco, temperatura zerowej wytrzymałości

### 1. INTRODUCTION

Main goal of this article is to invest formability, i.e. hot strength and hot plastic properties of alloy Invar 36. This Invar alloy contains 36 % of Ni and it is known for its extremely low thermal expansion, which almost equal to zero. Due to this property it is used for applications, where dimensional stability under the influence of temperature changes is needed. This ability determines this alloy as one of the best alloys to use for precision instruments, magnetic rectifiers, relays, transformer sheets, dynamo sheets, radio and electronic equipment, aircraft equipment, optical and laser systems. In addition, this alloy can

be used for production of parts used for storage and transport of cryogenic fluids [1–5].

Formability is the ability of the body to plastic deformation under certain forming conditions until the formation of critical cracks or rupture. For the study of hot formability of metal materials, tensile or torsion test made by plastometers can be used [6–9]. In this study the formability of Invar 36 alloy was tested by hot continuous tensile tests up to rupture, which have been made by plastometer HDS-20 in wide range of temperatures and stroke rates.

Based on the results obtained by the tests, 3D maps have been constructed. These maps show dependence of the contractual hot ultimate tensile

**Corresponding Author:** Petr Kawulok, email: petr.kawulok@vsb.cz  
VŠB – Technical University of Ostrava, Faculty of Materials Science and Technology,  
17. listopadu 2172/15, 708 00 Ostrava – Poruba, Czech Republic

strength, hot ductility and hot reduction of area on the deformation temperature and mean strain rate. Advantage of 3D maps is the possibility to predict strength and plastic properties of investigated material in dependence of the thermomechanical conditions of forming [10, 11]. Based on the obtained results the nil-ductility temperature of the investigated alloy will be determined. The nil-ductility temperature  $NDT$  ( $^{\circ}\text{C}$ ) corresponds to the temperature of zero ductility (100% brittleness of material) during tensile tests with direct heating to the deformation temperature [12–14]. Moreover, the nil-strength temperature  $NST$  ( $^{\circ}\text{C}$ ) will be determined too. This temperature is defined as a temperature, at which metal materials lost their strength due to the melting of grain boundaries during the heating. It means that materials cannot withstand any load at this temperature. The nil-strength temperature is important parameter for investigation of brittleness, respectively sensitivity to cracking of metal materials at very high temperatures [12–16].

## 2. EXPERIMENT DESCRIPTION

The Invar 36 alloy was delivered, as a rods with diameter 10 mm, in the initial state after cold drawing and annealing. Chemical composition of invar 36 is shown in Table 1.

**Table 1. Chemical composition of the Invar 36 alloy in wt. %**

**Tabela 1. Skład chemiczny stopu Invar 36 w % wag.**

C	Si	Mn	Co	Ni	Fe
0.043	0.15	0.40	0.013	36.01	63.38

By using of hot tensile tests, which were performed on the HDS-20 simulator, the hot strength and plastic properties of Invar 36 alloy were experimentally determined.

In the first phase of experiment, the nil-strength temperature of investigated alloy was measured by using special tensile test. For these purposes, the cylindrical specimens with diameter of 6 mm and length of 81 mm were made. The specimens were heated by electrical resistance heating by rate  $20^{\circ}\text{C}\cdot\text{s}^{-1}$  until  $1100^{\circ}\text{C}$  and then were slowly heated by rate  $2^{\circ}\text{C}\cdot\text{s}^{-1}$  from temperature  $1100^{\circ}\text{C}$  up to their rupture. A small constant tensile force of 80 N was applied to the specimens during the whole test. Temperature was measured by platinum thermocouples of type R, which were welded on surface in the middle of specimens length. From the reason of elimination of formation a scales on surface of specimens, all these test were performed in a vacuum environment which was approximately  $1.333\cdot 10^{-6}$  bar. To avoid influence of possible inhomogeneity this test was performed 3 times. Average value of nil-strength temperature was determined.

Formability, resp. hot plastic and hot strength properties of Invar 36 alloy were investigated by

hot continuous tensile tests up to rupture. For these purposes a cylindrical specimens with diameter of 10 mm and length of 116.5 mm (with threads at its ends) were made from the investigated alloy. These specimens were caught by jaws (made from stainless steel with partial contact area) and then these specimens were heated by simulator HDS-20 by electric resistance heating by rate of  $10^{\circ}\text{C}\cdot\text{s}^{-1}$  direct up to the deformation temperature. The deformation temperatures were selected in the range  $800\text{--}1390^{\circ}\text{C}$ . After 4 minutes dwell time on the selected deformation temperature specimens were deformed by tensile until the rupture during the constant stroke rate of  $1\text{ mm}\cdot\text{s}^{-1}$ ;  $30\text{ mm}\cdot\text{s}^{-1}$  and  $1000\text{ mm}\cdot\text{s}^{-1}$ . Temperature was measured by thermocouple, which were welded on a surface in the middle of tested specimens length. For tests with deformation temperatures above  $1250^{\circ}\text{C}$  platinum thermocouples of type R were used and for other tests thermocouples of type K were used. To eliminate a formation of scale during the heating, vacuum was used as well as in the case of tests for investigation of nil-strength temperature. The vacuum in testing chamber reach approximately  $1.333\cdot 10^{-6}$  bar.

## 3. PROCESSING OF MEASURED DATA

Experimentally determined nil-strength temperature corresponds to the highest registered value of temperature in the moment of sample break (caused by combination of the melting of grain boundaries and due to effect of very low tensile strength). This phenomenon is easy to recognize, because its association with steep decrease of temperature (Fig. 1). From the measured nil-strength temperature of investigated alloy, its mean value  $NST_{(\text{mean})} = 1419^{\circ}\text{C}$  (standard deviation of  $5.9^{\circ}\text{C}$ ) was determined. Determined nil-strength temperature of Invar 36 alloy corresponds to the temperature of solid  $1439^{\circ}\text{C}$ , which have been calculated by software JMatPro. The statistical assumption, that the nil-strength temperature

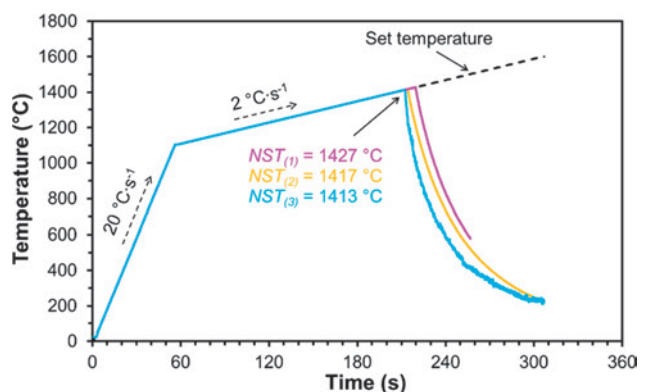


**Fig. 1. The measured nil-strength temperature of the Invar 36 alloy**

**Rys. 1. Zmierzona temperatura zerowej wytrzymałości stopu Invar 36**

of investigated alloy is lower than the solidus temperatures, has been proved [12, 13, 17].

Based on the data measured by a hot continuous tensile tests up to rupture the tensile diagrams were constructed, which show dependence of measured force on elongation of tested specimen (see example in Fig. 2).

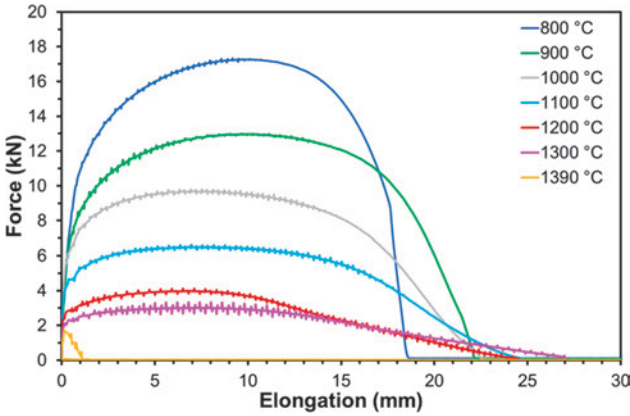


Fig. 2. Selected tensile diagrams of Invar 36 alloy – stroke rate  $30 \text{ mm}\cdot\text{s}^{-1}$

Rys. 2. Wybrane wykresy rozciągania stopu Invar 36 – częstotliwość uderzeń  $30 \text{ mm}\cdot\text{s}^{-1}$

From the tensile diagrams a maximal value of force  $F_{\max}$  (kN) and total elongation to the rupture  $\Delta L$  (mm) can be determined. These parameters together with initial cross-section of the tested specimens  $S_0$  ( $\text{mm}^2$ ) and initial length  $L_0 = 20$  mm (in the case of used stainless steel jaws and dimensions of tested specimens) can be then used for the calculation of the contractual hot ultimate tensile strength  $UTS_H$  (MPa) and hot ductility  $D_H$  (%) of the investigated alloy [17]:

$$UTS_H = \frac{F_{\max} \cdot 1000}{S_0} \quad (1)$$

$$D_H = \frac{\Delta L}{L_0} \cdot 100 \quad (2)$$

The hot reduction of area  $RA_H$  (%) was expressed by cross-sectional areas of tested specimens after rupture  $S_1$  ( $\text{mm}^2$ ) and initial cross-section  $S_0 = 78.5 \text{ mm}^2$  [17]:

$$RA_H = \frac{S_0 - S_1}{S_0} \cdot 100 \quad (3)$$

From the strain intensity and from the stroke rate (for conditions of uniform deformation, i. e. until the formation of the neck), the mean strain rate  $\dot{\epsilon}_{\text{mean}}$  ( $\text{s}^{-1}$ ) was determined [17]:

$$\dot{\epsilon}_{\text{mean}} = 1.155 \frac{\ln\left(\frac{0.5\Delta L}{L_0}\right)}{(0.5\Delta L) - L_0} v_{\text{stroke}} \quad (4)$$

For the stroke rate  $v_{\text{stroke}} 1 \text{ mm}\cdot\text{s}^{-1}$  the mean strain rate was equal to  $0.09 \text{ s}^{-1}$ , in the case of stroke rate  $30 \text{ mm}\cdot\text{s}^{-1}$  the mean strain rate was equal to  $2.5 \text{ s}^{-1}$  and

in the case of stroke rate  $1000 \text{ mm}\cdot\text{s}^{-1}$  the mean strain rate was equal to  $75 \text{ s}^{-1}$ .

The contractual hot ultimate tensile strength of investigated alloy Invar 36 was in fact increasing with decreasing of deformation temperature and with increasing of mean strain rate, respectively with increasing of stroke rate (Fig. 3). Around deformation temperature of  $1150 \text{ }^\circ\text{C}$  it is possible to observe for each mean strain rate change of trend in dependence of the contractual hot ultimate tensile strength on deformation temperature. The highest value of the contractual hot ultimate tensile strength was reached, when mean strain rate was  $75 \text{ s}^{-1}$  and deformation temperature  $800 \text{ }^\circ\text{C}$ .

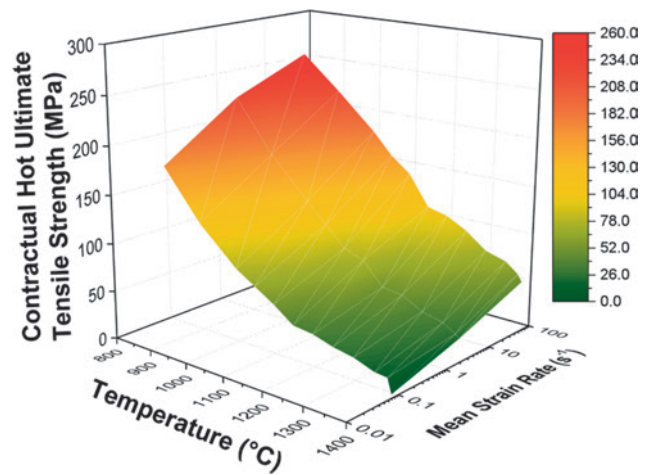


Fig. 3. 3D map of the contractual hot ultimate tensile strength of the Invar 36 alloy

Rys. 3. Mapa 3D wytrzymałości na rozciąganie na gorąco stopu Invar 36

Influence of deformation temperature and mean strain rate on hot plastic properties of investigated alloy are shown (Fig. 4 and Fig. 5). The hot ductility and the hot reduction of area of the Invar 36 alloy were increasing with increasing temperature until the maximum. After the maximum had been reached, steep decrease of these properties followed. For mean strain rate  $2.5 \text{ s}^{-1}$  a  $75 \text{ s}^{-1}$  showed investigated alloy the highest plastic properties at temperature  $1300 \text{ }^\circ\text{C}$ . For mean strain rate of  $0.09 \text{ s}^{-1}$  was the highest hot ductility and hot reduction of area measured at temperature  $1050 \text{ }^\circ\text{C}$ . At deformation temperatures higher than  $1350 \text{ }^\circ\text{C}$  overheating and subsequent burning of structure of investigated alloy probably occurred, which caused steep decrease of hot ductility and hot reduction to zero (Fig. 4 and Fig. 5).

Based on the results of continuous hot tensile test up to rupture the nil-ductility temperature  $NDT = 1390 \text{ }^\circ\text{C}$  was determined. This temperature corresponds to the temperature, where the plastic properties of investigated alloy are almost zero. For investigated alloy Invar 36 is  $NDT$  lower than  $NST_{(\text{mean})}$  by  $29 \text{ }^\circ\text{C}$ . This fact corresponds to the results of works [14, 17, 18], where were determined the difference

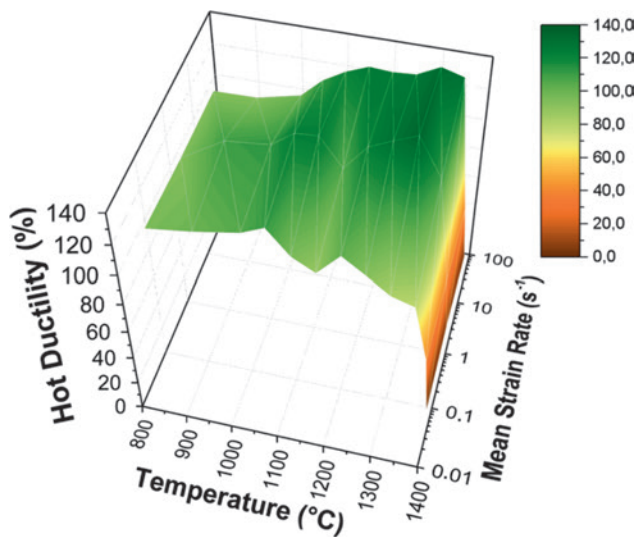


Fig. 4. 3D map of the hot ductility of the Invar 36 alloy  
 Rys. 4. Mapa 3D plastyczności na gorąco stopu Invar 36

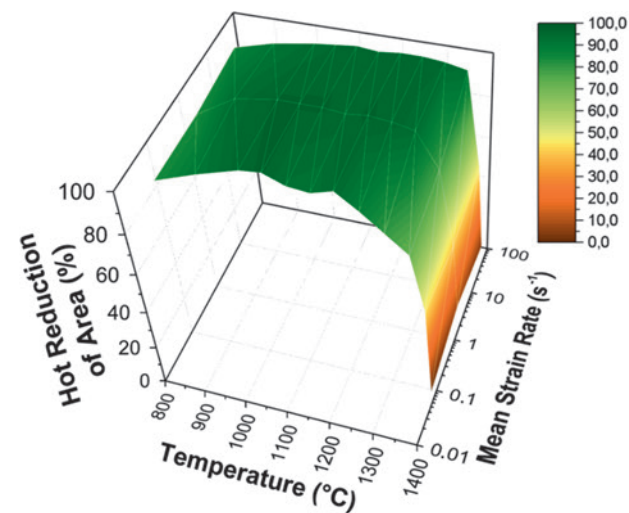


Fig. 5. 3D map of the hot reduction of area of the Invar 36 alloy  
 Rys. 5. Mapa 3D gorącej redukcji powierzchni stopu Invar 36

between the nill-strength temperature and nil-ductility temperature of investigated alloys in average 31 °C (with deviation ±8 °C).

#### 4. DISCUSSION OF RESULTS

From the point of view of formability it is interesting to observe local decrease of plastic properties of Invar 36 alloy in the range of temperature 1100–1200 °C (Fig. 4 and Fig. 5). At the temperature of 1150 °C and strain rate of 0.09 s<sup>-1</sup> hot ductility decreased to 80 % and hot reduction of area decreased to 92 %. This decrease of plastic properties is not large, especially in the case of hot reduction of area, but on the other hand it is not so insignificant (especially in the case of hot ductility).

To investigate this kind of local decrease of plastic properties around the deformation temperature of

1150 °C, structural state of Invar 36 alloy after heating to selected temperatures (1000 °C, 1100 °C, 1150 °C and 1200 °C) was additionally investigated. Prepared cylindrical specimens (diameter 10 mm, length 15 mm) were after heating to the selected temperature and after subsequent 5 minutes dwell time quenched in water. To make process of etching of grain boundaries of initial grain boundaries easier, all samples were annealed in an electric resistant furnace at 200 °C for 10 minutes followed by cooling on air. The specimens were then metallographically analyzed (in cross-section in the middle of their height), by using of standard optical microscopy. In all cases, the structure of the Invar 36 alloy consisted of austenite after heating to selected temperatures (see examples in Fig. 6). Metallographic analysis of investigated alloy (after heating to selected temperatures) did not show any structural elements or phases, which could be responsible for this local decrease of plastic properties. This fact was confirmed by an additional simulation of heating of Invar 36 alloy, which was made by software JMatPro (Fig. 7).

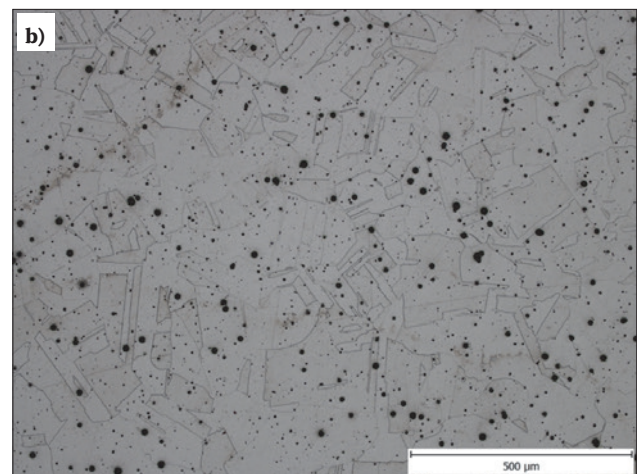
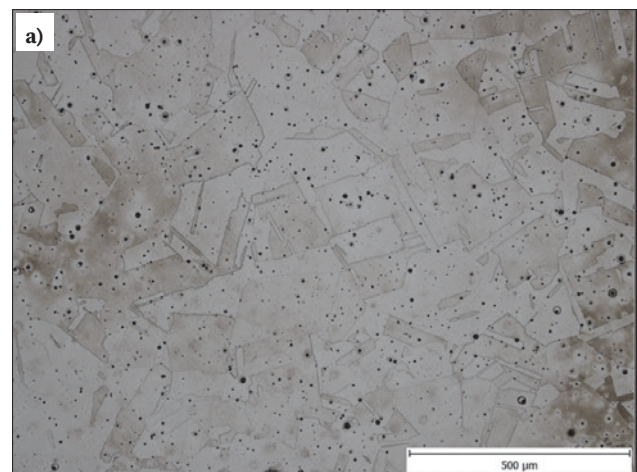


Fig. 6. Initial structure of investigated alloy after heating to selected temperatures: a) temperature of 1100 °C, b) temperature of 1150 °C

Rys. 6. Początkowa struktura badanego stopu po podgrzaniu do wybranych temperatur: a) temperatura 1100 °C, b) temperatura 1150 °C

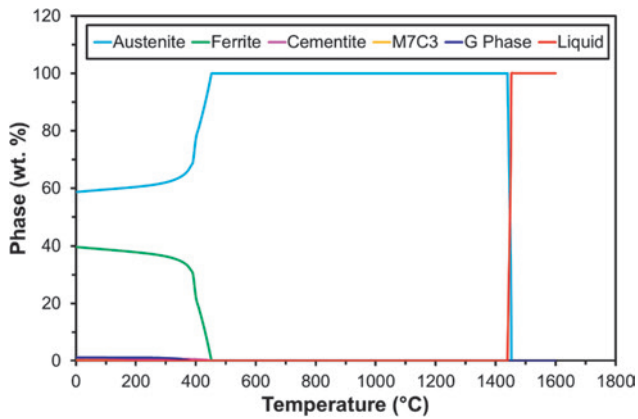


Fig. 7. Phase composition of Invar 36 alloy depending of temperature

Rys. 7. Skład fazowy stopu Invar 36 w zależności od temperatury

Metallographic analysis and mathematical simulation of heating did not show (at temperatures from 1000 °C to 1200 °C) any other structural phase than austenite, which may be responsible for the local decrease of plastic properties of investigated alloy around 1150 °C.

The decrease in plastic properties around the temperature 1150 °C was also observed in paper [19], where the hot formability of cast FeNi36 (equivalent name for Invar 36 alloy) alloy was investigated. In this case, continuous tensile tests up to rupture were made by plastometer Gleeble 3800 to investigate plastics properties of tested alloy. Prepared specimens were heated to the temperature 1350 °C and after delay at this temperature were these specimens cooled to the selected deformation temperatures (800–1200 °C). Comparison of plastics properties, resp. the values of the hot reduction of area in this paper (at mean strain rate was 0.09 s<sup>-1</sup>) with results presented in paper [19] (at mean strain rate 0.01 s<sup>-1</sup>) are shown below on Fig. 8.

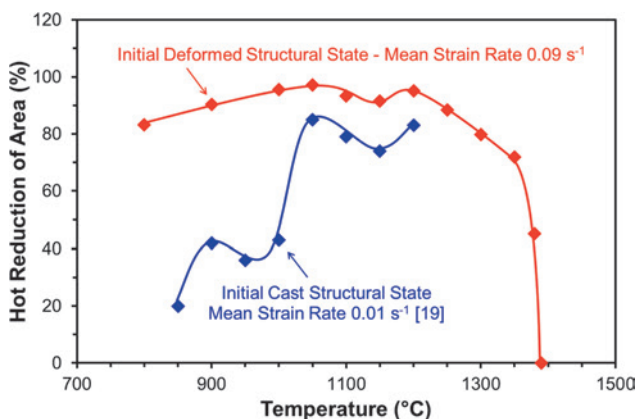


Fig. 8. Comparison of determined values of the hot reduction of area with the results of work [19]

Rys. 8. Porównanie wyznaczonych wartości ubytku powierzchni na gorąco z wynikami pracy [19]

From the graph shown in Fig. 8 is obvious, that in the case of investigated alloy in the initial cast state a local decrease of the hot reduction area around the

temperature 1150 °C is visible. Unfortunately, in paper [19] was these phenomena not explained. From Fig. 8 is obvious (even with considering small difference in strain rates at which both sets of tensile tests were performed) that formability of investigated alloy is lower for cast structural state than for deformed structural state. At lower deformation temperatures, the difference between the formability of the investigated alloy in the cast structural state and in the deformed structural state is considerable (approx. 40–60 %). It corresponds to general expectations that the coarse-grained cast structure negatively affects the formability of tested material in comparison to fine-grained deformed structure, because it should slow the nucleation phase of recrystallization and because of its contribution to intercrystalline fractures [20]. Fine-grained (deformed) structure should have higher formability at higher temperatures due to the limited development of intercrystalline fractures, associated to grain boundary sliding and acceleration of process of dynamic recrystallization [21, 22]. By recrystallization grain boundaries are changed and microcracks are moved from grain boundaries into the grain. In this intergranular position, the conditions for microcrack spreading are reduced [20].

In datasheet [5] it is shown, that in case of Invar 36 alloy forming temperatures should be 1090–1180 °C. It corresponds to the results of paper [19], where plastic properties of cast Invar 36 in hot conditions were investigated. The results set out in this presented article (Fig. 4 and Fig. 5) documented, that Invar 36 alloy in the initial deformed structural state reports, relatively good plastic properties in the range of investigated mean strain rates between temperatures 800 °C (on average  $D_H = 93\%$  and  $RA_H = 85\%$ ) and 1250 °C (on average  $D_H = 116\%$  and  $RA_H = 93\%$ ). From given comparison is obvious, that for forming of Invar 36 alloy in initial cast structural state is suitable range of deformation temperatures 1090–1180 °C, whereas in case of initial deformed structural state is suitable range of deformation temperatures wider 800–1250 °C. Of course, that with decreasing deformation temperature it is necessary to consider higher deformation resistance of investigated alloy, which was in this case expressed by contractual hot ultimate tensile strength.

## 5. CONCLUSIONS

By using of special tensile tests with constant loading of tested specimen during the continuous heating, the nil-strength temperature of Invar 36, which value is 1419 °C was found.

By using of continuous hot tensile tests up to rupture, the hot plastic and hot strength properties of Invar 36 alloy in the wide range of deformation temperatures 800–1390 °C and mean strain rates 0.09–75 s<sup>-1</sup> were investigated. Based on the results

of hot tensile tests until the rupture, 3D maps of the contractual hot ultimate tensile strength, the hot ductility and the hot reduction of area in dependence to the deformation temperature and mean strain rate were constructed. The Invar 36 alloy reached the highest ductility at the mean strain rate  $2.5 \text{ s}^{-1}$  or  $75 \text{ s}^{-1}$  at temperature  $1300 \text{ }^\circ\text{C}$ . For the mean strain rate  $0.09 \text{ s}^{-1}$  the highest ductility was observed at temperature  $1050 \text{ }^\circ\text{C}$ . The nil-ductility temperature, when the plastic properties of investigated alloy are almost equal to zero, was  $1390 \text{ }^\circ\text{C}$ . The nil-ductility temperature is lower than nil-strength temperature by  $29 \text{ }^\circ\text{C}$ .

From the point of view of formability, an interesting decrease in plastic properties was found for the Invar 36 alloy around the temperature  $1150 \text{ }^\circ\text{C}$ . Unfortunately, no other phases except austenite were found by metallographic analysis of specimens heated to the selected deformation temperatures or by simulations in JMatPro. The absence of other structural phases does not explain local decrease of plastic properties around the temperature  $1150 \text{ }^\circ\text{C}$ . Similar

decrease of plastic properties around the temperature  $1150 \text{ }^\circ\text{C}$  was presented in article [19], but these phenomena was not explained.

From the obtained results it is evident that the Invar 36 alloy in the initial deformed structural state shows relatively good plastic properties in the investigated range of mean strain rates at the temperatures from  $800 \text{ }^\circ\text{C}$  to  $1250 \text{ }^\circ\text{C}$ .

### Acknowledgements

The article was created thanks to the project No. CZ.02.1.01/0.0/0.0/17\_049/0008399 from the EU and CR financial funds provided by the Operational Programme Research, Development and Education, Call 02\_17\_049 Long-Term Intersectoral Cooperation for ITI, Managing Authority: Czech Republic – Ministry of Education, Youth and Sports and within the students' grant projects SP2022/73 supported at the VŠB – TU Ostrava by the Ministry of Education, Youth and Sports of the Czech Republic.

### REFERENCES

- [1] M. Yakout, M.A. Elbestawi, S.C. Veldhuis. A study of thermal expansion coefficients and microstructure during selective laser melting of Invar 36 and stainless steel 316L. *Additive Manufacturing*, 2018, 24, p. 405-418.
- [2] K. Wei, Q. Yang, B. Ling, X. Yang, H. Xie, Z. Qu, D. Fang. Mechanical properties of Invar 36 alloy additively manufactured by selective laser melting. *Materials Science and Engineering: A*, 2020, 772, article no. 138799.
- [3] Y. Yu, W. Chen, H. Zheng. Effects of Ti-Ce refiners on solidification structure and hot ductility of Fe-36Ni invar alloy. *Journal of Rare Earths*, 2013, 31 (9), p. 927-932.
- [4] K. Tirsatine, H. Azzeddine, T. Baudin, A. L. Helbert, F. Brisset, B. Alili, D. Bradai. Texture and microstructure evolution of Fe-Ni alloy after accumulative roll bonding. *Journal of Alloys and Compounds*, 2014, 610, p. 352-360.
- [5] High Temp Metals, Inc. Invar 36® Technical Data, [no date]. [Online] Available at: <https://www.hightempmetals.com/tech-data/hitempInvar36data.php> [Accessed on: 8 June 2022].
- [6] K. Dou, Q. Liu, Y. Zhou. Influence of boron addition on the hot ductility of medium carbon spring steel. *Engineering Failure Analysis*, 2021, 129, article no. 105696.
- [7] J. Yu, S. Zhang, H. Li, Z. Jiang, H. Feng, P. Xu, P. Han. Influence mechanism of boron segregation on the microstructure evolution and hot ductility of super austenitic stainless steel S32654. *Journal of Materials Science & Technology*, 2022, 112, p. 184-194.
- [8] L. Xing, Z. Zhang, Y. Bao. Hot ductility behavior of medium carbon sulfur-containing alloy steel. *Journal of Materials Research and Technology*, 2022, 19, p. 1367-1378.
- [9] P. Kawulok, P. Opěla, T. Kubina, I. Schindler, J. Bořuta, K.M. Čmiel, S. Ruzs, M. Legerski, V. Šumšal. Deformation behaviour of low-alloy steel 42CrMo4 in hot state. In: *Metal 2011, 20th International Conference on Metallurgy and Materials*. Brno, 18–20 May 2011, p. 350-356.
- [10] S. Ruzs, I. Schindler, K. Hrbáček, P. Kawulok, R. Kawulok, P. Opěla. An investigation of the deformation behaviour of the nickel alloys IN 713 LC and MAR M-247. In: *Metal 2015, 24th International Conference on Metallurgy and Materials*. Brno 3–5 June, p. 403-408.
- [11] P. Kawulok, I. Schindler, R. Kawulok, S. Ruzs, P. Opěla, J. Kliber, M. Kawuloková, Z. Solowski, K. M. Čmiel. Plasticometric study of hot formability of hypereutectoid C - Mn - Cr - V steel. *Metallurgija*, 2016, 55 (3), p. 365-368.
- [12] S. Tabaie, D. Shahriari, C. Plouze, A. Devaux, J. Cornier, M. Jahazi. Hot ductility behavior of AD730™ nickel-base superalloy. *Materials Science and Engineering: A*, 2019, 766, article no. 138391.
- [13] P. Kawulok, I. Schindler, B. Smetana, J. Moravec, A. Mertová, L. Drozdová, R. Kawulok, P. Opěla, S. Ruzs. The Relationship between Nil-Strength Temperature, Zero Strength Temperature and Solidus Temperature of Carbon Steels. *Metals*, 2020, 10 (3), article no. 399.
- [14] L. Kuzsella, J. Lukács, K. Szücs. Nil-strength Temperature and Hot Tensile Tests on S960QL High-strength Low-alloy Steel. *Production Processes and Systems*, 2013, 6 (1), p. 67-78.
- [15] S.T. Mandziej. Physical Simulation of Metallurgical Processes. *Materials and Technology*, 2010, 44 (3), p. 105-119.
- [16] T. Böllinghaus, H. Herold. *Hot Cracking Phenomena in Welds*. Berlin Heidelberg: Springer-Verlag, 2005.
- [17] R. Kawulok, I. Schindler, H. Navrátil, V. Ševčák, J. Sojka, K. Konečná, B. Chmiel. Hot formability of heat-resistant stainless steel X15CrNiSi 20-12. *Archives of Metallurgy and Materials*, 2020, 65 (2), p. 727-734.
- [18] S. Sawicki, H. Dyja, A. Kawalek, M. Knapinski, M. Kwapisz, K. Laber. High-temperature characteristics of 20MnB4 and 30MnB4 micro-addition cold upsetting steels and C45 and C70 high-carbon-steels. *Metallurgija*, 2016, 55(4), p. 643-646.
- [19] Y. Yu, W. Chen, H. Zheng. Effects of Ti-Ce refiners on solidification structure and hot ductility of Fe-36Ni invar alloy. *Journal of Rare Earths*, 2013, 31 (9), p. 927-932.
- [20] M. Židek. *Metallurgická tvaritelnost ocelí za tepla a za studena [Hot and cold metallurgical formability of steels]*. Praha: Aleko, 1995.
- [21] Z. Wang, S. Sun, B. Wang, Z. Shi, R. Zhang, W. Fu. Effect of Grain Size on Dynamic Recrystallization and Hot-ductility Behaviors in High-nitrogen CrMn Austenitic Stainless Steel. *Metallurgical and Materials Transaction A*, 2014, 45 (8), p. 3631-3639.
- [22] J. Li, B. Jiang, Ch. Zhang, L. Zhou, Y. Liu. Hot embrittlement and effect of grain size on hot ductility of martensitic heat-resistant steels. *Materials Science and Engineering A*, 2016, 677, p. 274-280.